A zero-field examination of transverse spin freezing (Invited)

D.H. Ryan[1], J. van Lierop[1], M.E. Pumarol[1], M. Roseman[1] and J.M. Cadogan[2]

[1] *Physics Department and Centre for the Physics of Materials, McGill University, 3600 University Street, Montreal, Quebec H3A 2T8, Canada*

[2] *School of Physics, The University of New South Wales, Sydney, NSW 2052, Australia*

(October 6, 2000)

Zero-field μSR has been used to study transverse spin freezing in $a-\mathrm{Fe_xZr_{100-x}}$ and $a-\mathrm{Fe_{90-x}Ru_xZr_{10}}$. The derived phase diagrams, while generally consistent with model calculations, exhibit some significant differences. Comparison with applied field measurements shows that T_{xy} is strongly affected by a field and falls as B^{-1}, contrary to mean field predictions.

76.75.+i 75.50.Bb 75.50.Lk 75.50.Kj

I. INTRODUCTION

T_{xy} marks the point on cooling a partially frustrated ferromagnet where $xy-$spin-glass order develops in the plane perpendicular to the ferromagnetic order established at T_c. Below T_{xy}, both types of order co-exist uniformly throughout the material. The phenomenon results from a delicate balance, much as the liquid does in P-V-T systems: frustration must be present or only ferromagnetic order is observed, while too much frustration leaves only the spin-glass.

Transverse spin freezing is observed in a wide variety of experimental systems [1], and has been predicted by both mean field [2] and numerical [3] models of Heisenberg spin systems. The issues that remain therefore are (i) confirming that the experimental signatures observed are indeed those of transverse spin freezing, and not the result of other effects, and (ii) accurately testing and providing guidance to detailed theoretical models of the phenomenon. Many experimental techniques have been used to settle the first issue, while muon spin relaxation (μSR) is now making a substantial contribution to the second.

The most direct experimental evidence for transverse spin freezing has come from Mössbauer spectra collected on field cooling through T_{xy}. The magnetic field is used to orient the ferromagnetic order above T_{xy}, and then the ordering of components perpendicular to this order is detected through changes in line intensities in the Mössbauer spectrum. Data from **Au**Fe [4] and $a-$Fe-Zr alloys [5] have clearly confirmed the basic nature of the transition at T_{xy}. Furthermore, by exploiting the electric field gradient in crystalline **Au**Fe as an internally defined axis, it was possible to show that transverse spin freezing occurs spontaneously and does not require an external field to define the ferromagnetic ordering direction [6].

It is important to note that alternative explanations of the observations in terms of magnetic inhomogeneities, or clusters, can be ruled out by additional measurements. These cluster models [7] appeal to the presence of magnetically isolated regions that order at a temperature below that of the ferromagnetic matrix and lead to a breakdown of the ferromagnetic order established at T_c. However this description fails at two levels (i) there is no direct evidence for the presence of clusters, (ii) there is no loss of ferromagnetic order below T_{xy}. The uniformity of the ordering has been confirmed by careful analysis of Mössbauer spectra obtained in the vicinity of T_{xy} which set an upper limit of 0.5% on the fraction of iron atoms in $a-\mathrm{Fe_xZr_{100-x}}$ (at $x = 90$) that could be present in isolated clusters [5,8]. Similar limits were placed on the cluster concentration for $89 \leq x \leq 93$ using μSR [9]. However, it is the demonstration that long-range ferromagnetic order persists through T_{xy} down to 5 K (i.e. $\mathrm{T} < 0.1\ \mathrm{T}_{xy}$) [10] that ultimately allows us to dismiss cluster-based models. The ferromagnetic orders persists at all temperatures below T_c, and is only lost when the level of frustration becomes too high for ferromagnetic order to develop. The system is then never ferromagnetic and enters the spin glass state on cooling [11].

One problem limiting direct comparison between experiment and theory is that it is difficult to relate the simplified exchange and moment distributions assumed in the models to the essentially unknown distributions present in real materials. However, we can scale out these variables by constructing two dimensionless ratios: the first is a measure of the system's collinear order, the ratio between the magnetisation along the $z-$axis, M_z and the total moment S this ranges from one for a ferromagnet to zero for a spin glass. The second is the ratio of the transition temperatures ($\mathrm{T}_{xy}/\mathrm{T}_c$). Fig. 1 shows that this procedure yields close agreement between numerical simulations and experiment. Since the numerical and mean-field models both agree on the form of the expected phase diagram and provide a consistent description of transverse spin freezing, and the numerical model yields the correct scaling between the non-collinearity and the transition temperatures, it seems reasonable to proceed assuming that the basic phenomenology is established.

The work presented here concentrates on examining the detailed behaviour around T_{xy} and comparing it to existing theoretical models. Our starting point is the prediction by numerical simulations that transverse spin freezing should be associated with a significant fluctuation peak [3]. We have exploited the excellent sensitivity of μSR to both static and dynamic magnetic behaviour to demonstrate that this dynamic peak is indeed present and coincides with the expected growth in static order at T_{xy} [9,12,13]. The μSR measurements are made without having to apply an external field (c.f. the Mössbauer data above) and therefore provide an unperturbed window onto the ordering behaviour of partially frustrated magnetic systems.

Data on two related systems are presented. $a-Fe_xZr_{100-x}$ is a well-characterised, metallurgically stable, partially frustrated Heisenberg magnet [5]. It is ferromagnetic at x=88, and enters the fully frustrated spin-glass state at a critical concentration of $x_c \sim 94$ [5]. Neutron depolarisation has confirmed that at all compositions where ferromagnetic order is established at T_c, this order persists through T_{xy} and down to the lowest temperatures examined (~5 K) [10,11]. μSR has further shown that the magnetic order is uniform, with no evidence for magnetic segregation [9]. The system therefore provides an ideal test-bed for the study of transverse spin freezing. Applied-field Mössbauer studies have indicated the x_c is ~94, however recent zero-field μSR (ZF–μSR) work has placed the boundary below $x = 93$. We therefore concentrated our efforts on the $92< x \leq 93$ range in order to settle this discrepancy. Unfortunately, the critical composition for the loss of ferromagnetic order in $a-Fe_xZr_{100-x}$ lies at the limit of the glass forming region, precluding investigation of the behaviour significantly beyond x_c. To overcome this limitation, we turn to a ruthenium-doped series: $a-Fe_{90-x}Ru_xZr_{10}$ where $x_c = 2.5$ [11,13,14] and the glass is stable at least as far as $x = 20$ [15].

II. EXPERIMENTAL METHODS

Meter-length ribbons 1–2 mm wide of $a{-}Fe_xZr_{100-x}$ and $a-Fe_{90-x}Ru_xZr_{10}$ were prepared by arc-melting appropriate amounts of the pure elements (Fe 99.97%, Ru 99.9% and Zr 99.5%) under Ti-gettered argon, followed by melt-spinning in 40 kPa helium with a wheel speed of 55 m/s. Sample compositions were checked by electron microprobe and found to be ~0.1 at.% Fe-rich of nominal in all cases. The Ru-doped series exhibited some loss of ruthenium (typically 0.1 – 0.4 at.%), so actual, rather than nominal compositions are quoted here. Cu K_α x-ray diffraction on a conventional automated powder diffractometer, and room temperature ^{57}Fe Mössbauer spectra were used to confirm the absence of crystalline contamination.

Zero-field μSR (ZF–μSR) measurements were made on the M13 and M20 beamlines at TRIUMF. Sample temperature was controlled between 5 K and 300 K in a conventional He-flow cryostat. Field-zero was set to better than 0.01 mT using a Hall probe (M13) and to 1 μT using a flux-gate magnetometer (M20). Samples consisted of ~15 layers of $20\mu m$ thick ribbons clamped between copper rings to give thicknesses of 170–200 $\mathrm{mg\,cm^{-2}}$ over a 16 mm diameter active area. A pure silver (99.99%) mask [16] prevented stray muons from striking any of the mounting hardware. Essentially 100% spin polarised μ^+ were implanted with their moments directed in the backward direction (*i.e.* along z). The subsequent decay e^+ is emitted preferentially along the moment direction. The rotation of the μ^+ spin is conventionally followed by plotting the asymmetry (A) between scintillation detectors placed in the forward (F) and backward (B) directions relative to the initial μ^+ flight direction ($A = B - F/F + B$) as a function of time. Histograms containing 1–4 $\times 10^7$ events were acquired with timing resolutions of either 0.625 ns (well below T_c) or 1.25 ns (below T_c to 300 K). The time-dependent asymmetry was then fitted using a conventional non-linear least-squares minimisation routine to functional forms described below.

In addition, preliminary longitudinal-field muon spin relaxation (LF-μSR) measurements were made on $a-Fe_{92}Zr_8$ using the M20 beamline. Longitudinal fields (i.e. parallel to the initial muon polarisation) of up to 5.5 Tesla were applied using a superconducting solenoid. In all cases, the field was applied well above T_{xy} and the measurements made on field cooling, to eliminate any possible sample history effects.

III. DATA ANALYSIS

Many excellent descriptions of ZF–μSR exist [17] so for the purposes of the data described here we note only the following. The materials studied here are both structurally disordered (*i.e.* glassy) and magnetically disordered as a result of exchange frustration, therefore we expect a distribution of local fields to be present. For a system with an isotropic Gaussian distribution of static local fields, the asymmetry will follow the Kubo-Toyabe (K-T) form [18]:

$$G_z(\Delta, t) = \frac{1}{3} + \frac{2}{3}\left(1 - (\Delta t)^\alpha\right)\exp\left(-\frac{(\Delta t)^\alpha}{\alpha}\right)$$

where Δ/γ_μ is the rms field. This function (see insets to Fig. 2 at 110 K and 5 K) exhibits a minimum at $\Delta \times t = \sqrt{3}$ then recovers to $\frac{1}{3}$ for long times. We modeled the shallowing of the K-T minimum observed near T_c by introducing a scaling power α that serves to smoothly interpolate between the form expected for a

Gaussian distribution of fields ($\alpha = 2$) and a Lorentzian distribution ($\alpha = 1$) [19]. α was found to start close to one right at T_c but recovered to 1.8 ± 0.2 within 30 K below T_c. The asymptotic value of $\frac{1}{3}$ reflects the fact that on average, $\frac{1}{3}$ of the muons will have their moments parallel to the local field and therefore do not precess. Above T_c, there will be no magnetic order and hence no static field. However the presence of neighbouring moments that fluctuate in time will lead to a dephasing of the muon polarisation by a process analogous to spin-lattice relaxation in NMR (T_1) and an exponential decay of the asymmetry is observed:

$$A_d = A_o \exp\left(-(\lambda t)^{\beta}\right)$$

where λ is an effective relaxation rate. This stretched exponential gave an excellent fit to the data. β was generally close to one above T_c but fell as low as 0.3 immediately below T_c. In cases where both static order and fluctuations are present, the asymmetry decays according to the product of the two functions:

$$A = A_d \times G_z.$$

The data in Fig. 2 illustrate a primary strength of μSR: static and dynamic magnetic effects can be observed simultaneously and they are sufficiently well-separated in the data that they can be distinguished with great reliability. In Fig. 2, the static K-T contribution is confined to the first 20 ns, while the dynamic decay is spread over the remaining 5 μs.

IV. RESULTS AND DISCUSSION

Fig. 3 shows the temperature dependence of the static order for a range of compositions. It is immediately apparent that the ordering temperature falls with increasing iron content (x). In addition, there is a clear break in the temperature dependence of Δ in all but the $x = 93$ data. Δ(T) was modeled as the sum of two modified Brillouin functions [20] to reflect the successive ordering of first the longitudinal components at T_c followed by the transverse components at T_{xy}. While the increase in static order at T_{xy} is expected, it is not as convincing a demonstration of transverse spin freezing as the clear peak observed in the dynamics (Fig. 4). On cooling, λ diverges at T_c as the ferromagnetic order is established. Further cooling leads to a steady reduction in λ as magnons freeze out. However, there is a further increase at T_{xy}, and this peak is far clearer than the break in the slope of Δ(T). The data in Fig. 4 have been fitted with a Curie-Weiss divergence on cooling towards T_c and a Gaussian peak for the fluctuations at T_{xy}.

The fits to Δ(T) and λ(T) yield two estimates for each of T_c and T_{xy}. These are plotted, with our previous results on this system [12], in Fig. 5. As before, we obtain excellent agreement between the static and dynamic estimates of both T_c and T_{xy} by μSR and also with results from χ_{ac} and Mössbauer spectroscopy. The form of the phase diagram is consistent with the model predictions, and close examination of the behaviour around $x = 93$ shows that $x_c \sim 92.8$, significantly below that determined by applied field Mössbauer spectroscopy [5], but consistent with our earlier ZF–μSR [12] and depolarisation results [10]. However, two departures from expectations are apparent: (i) T_c is clearly a stronger function of composition than T_{xy}, and (ii) the Mössbauer values for T_{xy} lie well below those derived from μSR.

The first point is a significant departure from existing theoretical models. Both numerical [3] and mean-field [2] phase diagrams show a linear frustration dependence for both transitions. Even though we are varying composition rather than frustration, T_{xy} varies linearly while T_c declines much faster. This behaviour is even more marked in the $a-Fe_{90-x}Ru_xZr_{10}$ phase diagram (Fig. 6). Here, some of the decline in T_c could be attributed to a reduction in the Fe moment [21], and the average exchange in the Ru-doped system is clearly weaker as the transition temperature at x_c is nearly 40 K lower than in the binary system (Fig. 5). However, these differences should affect both T_c and T_{xy}, we therefore believe that the stronger composition dependence of T_c on approaching x_c in both systems represents a real departure from the theoretical predictions.

The second difference, systematically low Mössbauer values for T_{xy}, is only seen for the a–Fe-Zr data, while the values for the Ru-doped series are consistent with, or slightly above the corresponding μSR results. We attribute this difference to the manner in which the Mössbauer measurements were made. The a–Fe-Zr values were obtained in fields of 3–5 Tesla, while those for the Ru-doped series could be obtained in zero field, as the temperature dependence of the hyperfine field (B_{hf}(T)) [11] exhibits the same clear break in slope as Δ(T). These results strongly suggest that T_{xy} is reduced by an applied field, and serve to underline the need to study the effects of frustration in zero external field. They also explain why the Mössbauer estimate for x_c in a–Fe-Zr was too high. With T_{xy} systematically underestimated, the composition where T_c and T_{xy} are extrapolated to meet is shifted to larger x.

Given the severe effects of an applied field on T_{xy} (the value for $x = 92$ is reduced by a factor of two from its zero-field value) it is somewhat surprising that the scaling plot in Fig 1 works at all, as it combines results both with and without an external field and compares them with zero-field simulations. Since the scaling works, it implies that T_{xy}/T_c and M_z/S are strongly linked, even in an applied field, and that the track followed by the data in Fig 1 is a universal curve that holds whether the measurement is made with or without a field. This assertion should be readily accessible to investigation by numerical simulation.

Finally, in an attempt to quantify the effects of an applied field on T_{xy}, we have obtained preliminary μSR data in longitudinal fields of up to 5.5 Tesla [22]. We were able to observe a fluctuation peak at all fields used and thus followed T_{xy} as the field suppressed it by over a factor of four. Theoretical predictions for the functional form of this suppression are limited to mean-field models which predict a dependence of the form:

$$T_{xy}(B) \propto T_{xy}^0 \left(1 - \frac{B^x}{A}\right)$$

with x being 2 [2,23], 2/3 [2,24] or 1 [25]. Unfortunately, none of the three predicted forms describes the observed field dependence of T_{xy}. Preliminary analysis suggests that a function of the form:

$$T_{xy}(B) = T_{xy}^0 \left(1 - \frac{B}{(J_s + B)}\right)$$

fits the data quite well, making the power x in the first equation equal to -1, and yielding a severe disagreement with predictions.

V. CONCLUSIONS

ZF–μSR has been used to map out the phase diagrams of $a-Fe_xZr_{100-x}$ and $a-Fe_{90-x}Ru_xZr_{10}$, and the critical concentrations for the loss of ferromagnetic order have been found to be $x_c = 92.8$ and $x_c = 2.5$ respectively. While the basic form of the phase diagrams is consistent with existing models, the decline in T_c is more rapid than expected. Comparison with Mössbauer and μSR measurements in applied fields shows that T_{xy} is strongly suppressed and falls as B^{-1}, in direct conflict with mean field predictions.

This work was supported by grants from: the Natural Sciences and Engineering Research Council of Canada, Fonds pour la formation de chercheurs et l'aide à la recherche, Québec, the Australian Research Council and the Australian Nuclear Science and Technology Organisation. The authors would like to thank the TRIUMF μSR support staff for their invaluable help and advice.

[1] D.H. Ryan in "*Recent Progress in Random Magnets*" D.H. Ryan (ed.) p. 1–40, (1992), World Scientific Publishing Co. Pte. Ltd. (Singapore).

[2] M. Gabay and G. Toulouse, Phys. Rev. Lett. **47**, 201 (1981).

[3] J.R. Thomson, Hong Guo, D.H. Ryan, M.J. Zuckermann and M. Grant, Phys. Rev. **B45**, 3129 (1992).

[4] J. Lauer and W. Keune, Phys. Rev. Lett. **48**, 1850 (1982).

[5] H. Ren and D.H. Ryan, Phys. Rev. **B51**, 15885 (1995).

[6] R.A. Brand, J. Lauer and W. Keune, Phys. Rev. **B31**, 1630 (1985).

[7] S.N. Kaul, J. Phys.:CM **3** (1991), 4027.

[8] H. Ren, Ph.D. Thesis, McGill University, Montreal, Canada (1993).

[9] D.H. Ryan, J.M. Cadogan and J. van Lierop, J. Appl. Phys. **87**, 6525 (2000).

[10] D.H. Ryan, J.M. Cadogan and S.J. Kennedy, J. Appl. Phys. **79**, 6161 (1996).

[11] D.H. Ryan, Zin Tun and J.M. Cadogan, J. Magn. Magn. Mater. **177–81**, 57 (1998).

[12] D.H. Ryan, J.M. Cadogan and J. van Lierop, Phys. Rev. **B61**, 6816 (2000).

[13] D.H. Ryan, J.M. Cadogan and J. van Lierop, Phys. Rev. **B62**, 8638 (2000).

[14] D.H. Ryan, J.M. Cadogan and Zin Tun, J. Appl. Phys. **81**, 4407 (1997).

[15] V. Nagarajan, P.L. Paulose and R. Vijayaraghavan, J. de Phys. **49**, C8–1135 (1988). P.L. Paulose, V. Nagarajan, R. Krishnan, J. Voiron, H. Lassri, R. Nagarajan and R. Vijayaraghavan, J. Magn. Magn. Mater. **140–44**, 301 (1995).

[16] We confirmed that the silver used gave no time-dependent μSR signal down to 5 K.

[17] P. Dalmas de Réotier and A. Yaouanc, J.Phys.:CM **9**, 9113 (1997); A. Schenck and F.N. Gygax, in "Handbook of Magnetic Materials" vol. 9, K.H.J. Buschow (ed.) (Elsevier Science B.V., Amsterdam, 1995), p. 57.

[18] R. Kubo, Hyp. Int. **8**, 731 (1981). R. Kubo and T. Toyabe, in *Magnetic Resonance and Relaxation* edited by R. Blinc (North-Holland, Amsterdam, 1967), p. 810.

[19] Y.J. Uemura, T. Yamazaki, D.R. Harshman, M. Senba and E.J. Ansaldo, Phys. Rev. **B31**, 546 (1985); M.R. Crook and R. Cywinski, J. Phys.: Condens. Matter **9**, 1149 (1997).

[20] K. Handrich, Phys. Stat. Sol. **32**, K55 (1969).

[21] D.H. Ryan and J.M. Cadogan, J. Magn. Magn. Mater. **213**, 111 (2000).

[22] D.H. Ryan, J. van Lierop, M.E. Pumarol, M. Roseman and J.M. Cadogan, (unpublished results).

[23] G. Toulouse, M. Gabay, T.C. Lubensky and J. Vannimenus, J. de Phys. Lett. **43**, L-109 (1982).

[24] J.R.L. Almeida and D.J. Thouless, J. Phys. A **11**, 983 (1978).

[25] "*Spin Glasses*" by K.H. Fischer and J.A. Hertz, (Cambridge University Press, Cambridge, 1991), p. 319.

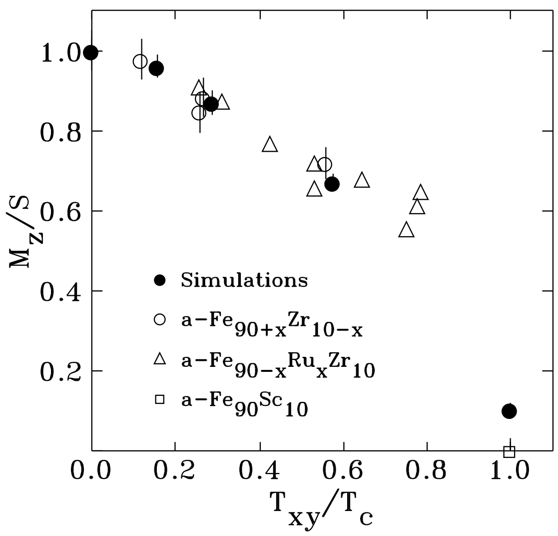

FIG. 1. Universal scaling plot showing the degree of non-collinearity (the ratio of the magnetisation, M_z, to the total moment S) plotted as a function of T_{xy}/T_c. The numerical simualtions [3] are in semi-quantitative agreement with data from a–Fe-Zr [5], Ru-doped a–Fe-Zr, and a–Fe-Sc which is a spin glass.

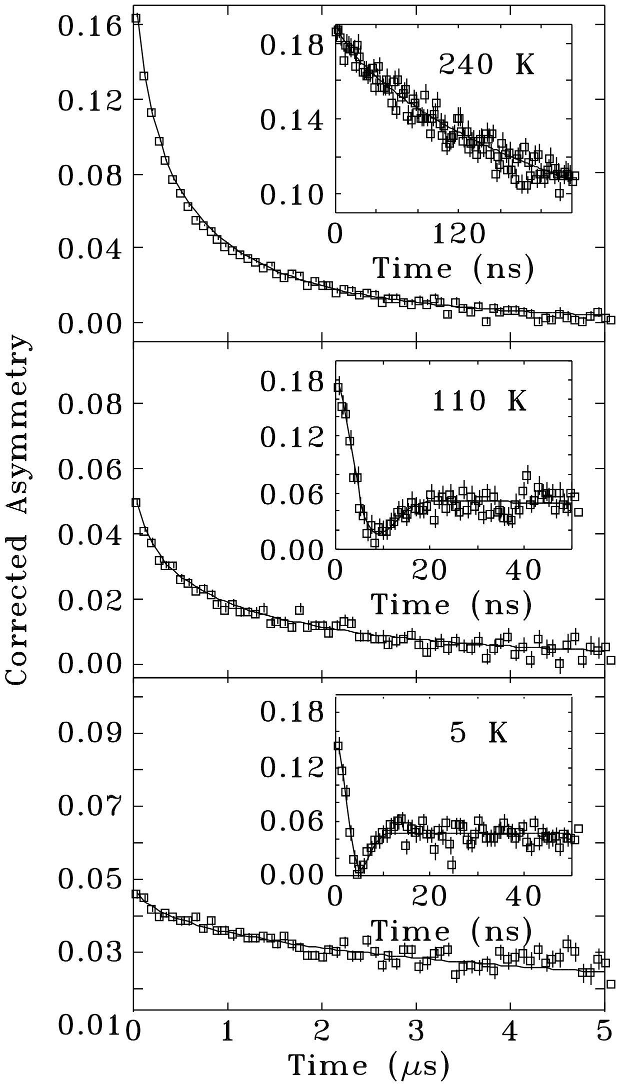

FIG. 2. Typical μSR patterns for a$-$Fe$_{91.5}$Zr$_{8.5}$ at 240 K (above T_c), 110 K (below T_c but above T_{xy}) and 5 K (below T_{xy}). Insets show the early time region of the data where, for $T < T_c$, the static K–T minimum is observed. Solid lines are fits to functions described in the text.

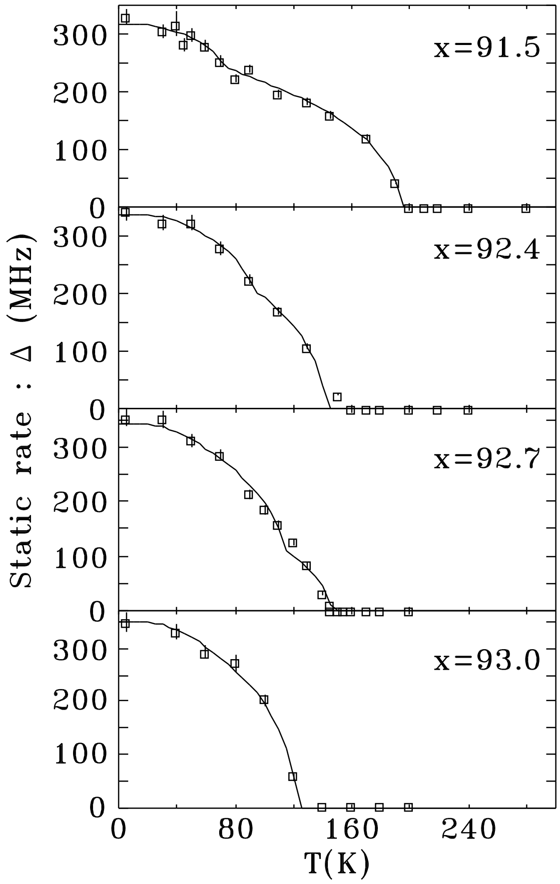

FIG. 3. Temperature dependence of the static relaxation rate (Δ) showing the steady reduction in ordering temperature with increasing frustration and the effects of transverse spin freezing. Solid lines are fits to a sum of two modified Brillouin functions described in the text.

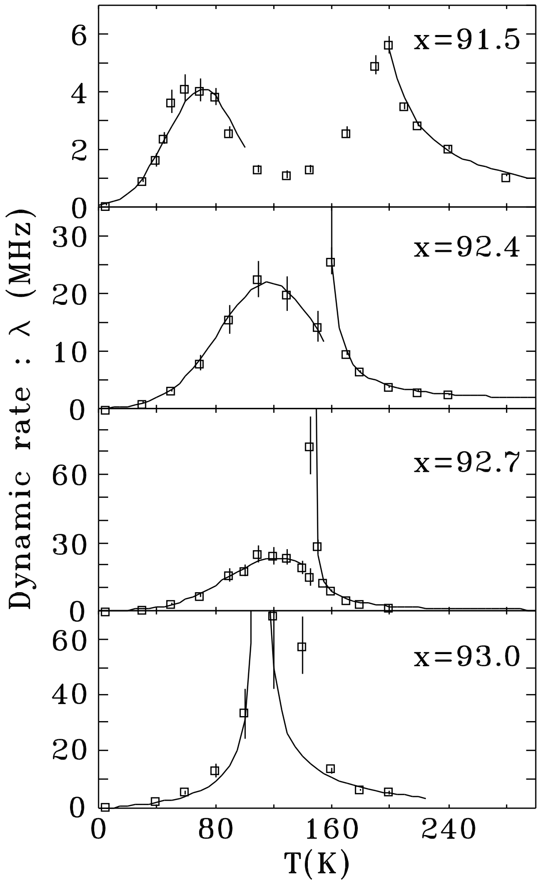

FIG. 4. Temperature dependence of the dynamic relaxation rate (λ) showing the high temperature divergence (T_c) merging with the lower temperature peak (T_{xy}) with increasing frustration. Solid lines show fits to a Curie-Weiss divergence at T_c and a gaussian fluctuation peak at T_{xy}.

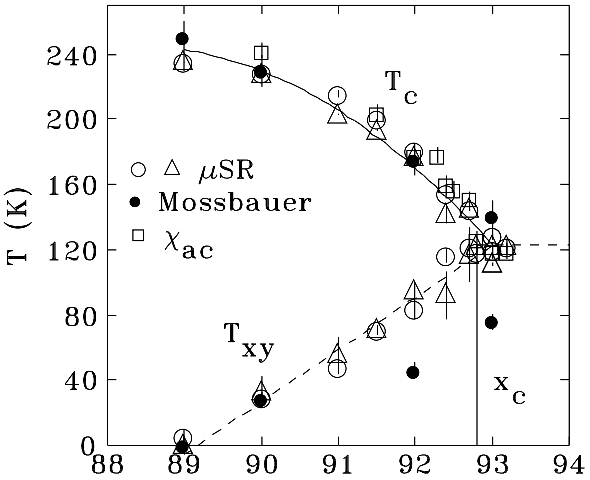

FIG. 5. Magnetic phase diagram for a$-Fe_xZr_{100-x}$ showing T_c and T_{xy} deduced from μSR data. T_cs derived from χ_{ac} measurements on the same samples are also shown as are T_c and T_{xy} values obtained on an independently prepared series of alloys measured using applied-field Mössbauer spectroscopy [5].

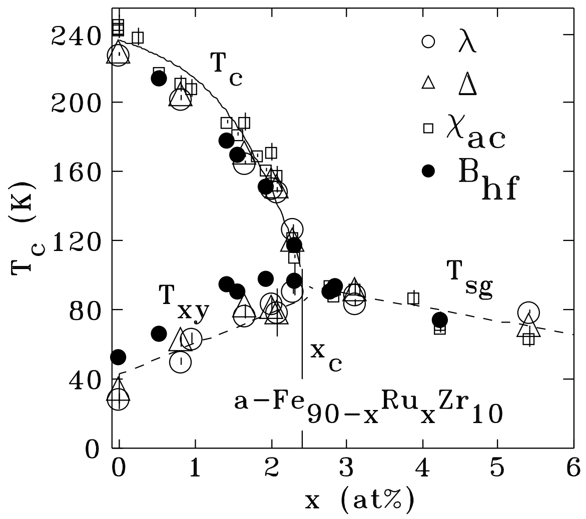

FIG. 6. Magnetic phase diagram for a$-Fe_{90-x}Ru_xZr_{10}$ showing T_c and T_{xy} deduced from μSR data. T_cs derived from χ_{ac} measurements on the same samples are also shown as are T_c and T_{xy} values obtained using Mössbauer spectroscopy.